Chemical Engineering Journal 155 (2009) 851–858

Contents lists available at ScienceDirect

Chemical Engineering Journal

journal homepage: www.elsevier.com/locate/cej

Role of nitrous acid decomposition in absorber and bleacher in nitric acid plant

N.D. Ingale, I.B. Chatterjee, J.B. Joshi*

Department of Chemical Engineering, Institute of Chemical Technology, University of Mumbai, Matunga, Mumbai 400019, India

ARTICLE INFO

Article history:
Received 16 September 2008
Received in revised form 8 September 2009
Accepted 9 September 2009

Keywords:
HNO_2 decomposition
HNO_2 oxidation with O_2
NO oxidation with HNO_3
Multi-component absorption and desorption with chemical reaction
HNO_3 and HNO_2 concentration profile in absorber
HNO_2 concentration profile in bleacher
NOx absorption

ABSTRACT

The stringent statutory regulation for clean environment makes the absorber and the bleacher in the nitric acid plant two very important equipments. The NOx finally released to the atmosphere from the absorber, is based on the mathematical calculations of the nitric acid and nitrous acid concentration profiles along the length of the absorber. The present work focuses on the role of HNO_2 decomposition in the absorber and the bleacher in the nitric acid plant. The decomposition of HNO_2 is a heterogeneous reaction resulting into the formation of nitric acid and desorption of nitric oxide. At high nitric acid concentration (40–50 wt.%), the reversibility of HNO_2 decomposition due to NO oxidation with nitric acid is important. The model for bleacher column is presented, which takes into account the de-colorization of the product acid from the absorption column and makes it free from the nitrous acid. The model for the bleacher also takes into account the decomposition and oxidation of HNO_2 with dissolved oxygen. The models proposed for absorber and bleacher are validated from the data collected from a mono-pressure nitric acid plant as well as the data present in open literature.

1. Introduction

Ever growing stringent statutory regulations for clean environment makes the absorption column in the nitric acid plant very important piece of equipment. The absorption column helps to achieve the desired strength of nitric acid as well as controls the emission of NOx gases. Considerable research efforts have produced a greater understanding [1–6] on the various aspects of NOx absorption, such as: (i) NOx gases consist of several components NO, NO_2, N_2O_3, N_2O_4, HNO_2, HNO_3, etc. and the liquid phase contains two oxyacids (i.e. nitric acid and nitrous acid), (ii) several reversible and irreversible reactions occur in both gas and liquid phases, (iii) absorption of multiple gases is accompanied by multiple chemical reactions, (iv) desorption of gases occur preceded by chemical reaction, (v) heterogeneous equilibria prevail between the gas and the liquid phase components, (vi) heat effects of the absorptions and the chemical reactions. Considerable modeling of various pieces of equipment of a nitric acid plant has been carried out and a modeling, simulation and optimization strategy has been proposed in a recent work by Chatterjee and Joshi [7]. In this work as well as practically by all the studies reported in the published literature [8–18], the depletion of aqueous nitrous acid in the absorber and the bleacher in a nitric acid plant has not been adequately modeled.

The depletion of nitrous acid in the aqueous solutions is an integral part of nitrogen oxide absorption from gas streams. In the bleacher, nitrous acid decomposes to nitric acid and also oxidation of nitrous to nitric acid occurs with the help of air. The decomposition of nitrous acid is a heterogeneous reaction resulting into the formation of nitric acid and the desorption of nitric oxide (NO). The nitric oxide desorbed then oxidizes in the environment of secondary air, which is passed into the bleacher as a side stream from the air compressor. The oxidation leads to the formation of NO_2, N_2O_3, N_2O_4, etc. which are further absorbed in nitric acid. The liquid phase HNO_2 and the dissolved NO can also get oxidized with dissolved oxygen. The process is therefore complex and an adequate mathematical model is essential to represent the various physico-chemical phenomena occurring in the absorption and bleacher processes.

Though the published literature has addressed the above mentioned (i)–(vi) components of the NOx absorption mechanism, two additional components need to be duly considered. These are: (a) kinetics of decomposition of HNO_2 and (b) the liquid phase oxidation of HNO_2 and NO. The objective is to obtain colorless and practically HNO_2 free nitric acid. The above mentioned two components have been included in the present work for the estimation of overall rate of reaction and have been used to model the absorber and bleacher units in a nitric acid plant.

2. Mathematical model

Except HNO_2 decomposition and oxidation, the NOx absorption has been duly addressed in the published literature [7,16]. The following discussion addresses HNO_2 decomposition and oxidation.

* Corresponding author. Tel.: +91 22 2414 0865; fax: +91 22 2414 5614.
E-mail address: jbj@udct.org (J.B. Joshi).

1385-8947/$ – see front matter © 2009 Elsevier B.V. All rights reserved.
doi:10.1016/j.cej.2009.09.017

Nomenclature

$\underline{a}$	interfacial area ($m^2\ m^{-3}$)
E_a	activation energy (J/mol K)
G	molar flow rate of inert (kmol s^{-1})
H_i	Henry's coefficient for species i (kmol m^{-3} kN m^{-2})
$[i]$	concentration of species i (kmol m^{-3})
k_1	forward rate constant for nitric oxide oxidation (kPa^{-1})
k_b	3rd order reaction rate constant in Eq. (10) ($kg\ m^{-2}\ s^{-1}\ Pa^{-1}$)
k'_b	reverse reaction rate constant in Eq. (11) ($kg\ m^{-2}\ s^{-1}\ Pa^{-1}$)
k_d	decomposition rate constant in Eq. (11) ($m^3\ kmol^{-1}\ s^{-1}$)
k	mass transfer coefficient in liquid (m s^{-1})
k_o	Arrhenius constant for Eq. (14)
K'	constant in Eq. (4)
K_n	equilibrium constant for Eqs. (30)–(33) (n = 2–5) ($kPa^{-2}\ s^{-1}$)
K_6	parameter defined by Eq. (25) ($kPa^{-1/2}$)
L	molar flow rate of water (kmol s^{-1})
p_i	partial pressure of gas phase species i (kPa)
P	operating pressure (kPa)
R	gas constant (kJ $kmol^{-1}\ K^{-1}$)
Ra_i	volumetric rates of mass transfer for species i (kmol $m^{-3}\ s^{-1}$)
R_d	rate of HNO_2 decomposition (kmol $m^{-3}\ s^{-1}$)
r_{NO}	rate of NO oxidation (kmol $m^{-3}\ s^{-1}$)
R_o	rate of HNO_2 oxidation (kmol $m^{-3}\ s^{-1}$)
S	cross-sectional area (m^2)
T	temperature of operation (K)
V	volume (m^3)
W_i	weight percent of species i
X^*_N	mole of reactive nitrogen per mole of water
Y_i	moles of species i per mole of inert
$Y^*_{H_2O}$	moles of water per mole of inert
Y^*_N	moles of reactive nitrogen per mole of inert
Y^*_{NO}	moles of divalent nitrogen per mole of inert
$Y^*_{O_2}$	moles of oxygen per mole of inert
z	length (m)

Greek letters

ε	hold-up

Subscripts

G	gas phase
L	liquid phase
n	stage number

Superscripts

b	heterogeneous equilibrium value
i	interface value
o	bulk gas phase

The overall equation for the liquid phase nitrous acid decomposition is given by:

$$3HNO_2(l) \overset{k_d}{\rightleftarrows} HNO_3(l) + 2NO(g) + H_2O(l) \quad (1)$$

The kinetics of nitrous acid decomposition has been studied by Abel and Schmid [19,20], and proposed the following rate expression assuming the N_2O_4 hydrolysis as the rate-determining step:

$$R_d = 3.93 \times 10^{-6} \left(\frac{[HNO_2]^4}{[NO]^2} \right) \quad (2)$$

Komiyama and Inoue [21] related the rate of HNO_2 depletion to the desorption rate of NO, by considering the N_2O_4 hydrolysis as the rate-determining step and presented in the form of following equation:

$$R_d = \frac{3}{2} k_L a [NO] \quad (3)$$

The liquid phase NO concentration is a function of the mass transfer characteristics of the equipment and HNO_2 concentration, which is obtained by combining Eqs. (2) and (3) as:

$$[NO] = 1.26 \times K' \times (k_L a)^{-1/3} [HNO_2]^{4/3} \quad (4)$$

Komiyama and Inoue [21] studied the decomposition kinetics by substituting Eq. (4) into Eq. (2) and the overall rate is thus given by:

$$R_d = k_d (k_L a)^{2/3} [HNO_2]^{4/3} \quad (5)$$

The value of k_d is $2.528 \times 10^{-2}\ m^3\ kmol^{-1}\ s^{-1}$ [21].

The decomposition of nitrous acid in aqueous solution is a complex phenomenon. The reaction (1) is considered to account for the depletion of nitrous acid. Substantial contribution in this field has led to the understanding of the following facts: (i) a critical concentration exists for strong solutions of nitrous acid, above which the rate of decomposition is very rapid and slower for concentrations below the critical value; (ii) the critical concentration is a function of temperature and pressure, and the value increases for low temperature and high pressure [22]; (iii) the reaction (1) is reversible [23], but the reverse reaction proceeds extremely slowly with dilute solutions of nitric acid [24,25]; (iv) the rate of chemical decomposition of the nitrous acid is practically doubled [23] for every 20 °C rise in temperature and (v) when nitric oxide gas is passed into nitric acid a greenish-blue solution is produced which shows the formation of nitrous acid [23] given by the following equation, which is reverse of Eq. (1):

$$2NO(g) + HNO_3(l) + H_2O(l) \rightleftarrows 3HNO_2(l) \quad (6)$$

In case of the absorber in the nitric acid plant, the NOx gases from oxidizer are introduced at the bottom tray and passed in the solution of nitrous and nitric acid on the tray. The calculation of absorption column starts at the bottom of the column. At the bottom plate, nitric acid concentration is high and it progressively decreases along the height of the column. Tereshchenko et al. [26] showed that, at lower temperatures and 50–60 wt.% HNO_3 concentrations, the liquid phase NO oxidation with HNO_3 (Eq. (6)) takes place according to following equation:

$$NO(g) + 2HNO_3(l) \overset{k_b}{\rightleftarrows} 3NO_2(g) + H_2O(l) \quad (7)$$

The mechanism proposed for liquid phase NO oxidation is as follows:

$$NO + HNO_3 \rightleftarrows HNO_3 \cdot NO \quad (8)$$

$$HNO_3 \cdot NO \rightleftarrows HNO_2 + NO_2 \quad (9)$$

The overall reaction can be represented by Eq. (7). The solubility of NO increases substantially, with an increase in the concentration of HNO_3 in the liquid phase and has been attributed to the formation of $[HNO_3 \cdot NO]$ associated group [27]. They also noted high concentration of $HNO_3 \cdot NO$ in the solution at HNO_3 concentrations between 55% and 60% HNO_3. The rate of NO oxidation with HNO_3 [26] can be written as:

$$r_{NO,L} = k_b (W_{HNO_3})^2 p_{NO} \quad (10)$$

The value of k_b is reported as 1.1694×10^{-10} kg m^{-2} s^{-1} Pa^{-1} [26]. Tereshchenko et al. [27] have also found that the rate of NO oxidation by nitric acid is very much higher than the rate of oxidation of NO by oxygen under the high nitric acid concentration (40–60 wt.%). Hence, it is necessary to account for the reverse reaction of HNO_2 decomposition given by Eq. (1) at nitric acid concentration in the range of 40–60 wt.%. The overall rate of HNO_2 decomposition can be written as:

$$R_d = k_d(k_L a)^{2/3}[HNO_2]^{4/3} - k'_b[HNO_3]^2[NO] \quad (11)$$

Chacuk et al. [28] have carried out experiments in stirred reactor at 13.3 rps and 50 dm^3/h of nitrogen gas through the nitrous acid solution and HNO_2 concentration was measured. The data reported by them also satisfies Eq. (3) with a $k_L a$ value of 2.613×10^{-3} s^{-1}.

Chacuk et al. [28] have further studied the HNO_2 oxidation with oxygen in liquid phase and the overall reaction is given by:

$$2HNO_2(l) + O_2(g) \xrightarrow{k_o} 2HNO_3(l) \quad (12)$$

When an inert gas passes through the solution of nitrous acid, then the decomposition of nitrous acid takes place as shown by reaction (1). If air replaces the inert gas then the nitrous acid oxidation also takes place as shown in Eq. (12) [28].

In the above overall reaction (12), NO oxidation with oxygen to NO_2, NO_2 dimerization to N_2O_4 and liquid phase HNO_2 decomposition were considered. The experiments were carried out by Chacuk et al. [28] for the study of HNO_2 oxidation kinetics, where HNO_3 concentration is below 10 wt.%. At such HNO_3 concentrations the oxidation of NO with HNO_3 is not important compared with NO oxidation by oxygen [27]. Hence, the reverse of reaction (1) is not considered.

Chacuk et al. [28] have determined the solubility of oxygen in liquid phase. The Henry's coefficient for oxygen is given by:

$$H_{O_2} = A_1(T) + A_2(T)W_{HNO_3} \quad (13)$$

where A_1 and A_2 are constants as defined in Chacuk et al. [28]

The rate equation for HNO_2 oxidation is given by:

$$R_o = k_o \exp\left(\frac{-E_a}{RT}\right)[HNO_2]^{1.61}[O_2] \quad (14)$$

The HNO_3 and HNO_2 formation takes place in the liquid phase by the absorption of various oxides of nitrogen in the liquid phase as shown in the following equations:

$$2NO_2(g) + H_2O(l) \rightarrow HNO_3(l) + HNO_2(l) \quad (15)$$

$$N_2O_3(g) + H_2O(l) \rightarrow 2HNO_2(l) \quad (16)$$

$$N_2O_4(g) + H_2O(l) \rightarrow HNO_3(l) + HNO_2(l) \quad (17)$$

$$HNO_2(g) \rightarrow HNO_2(l) \quad (18)$$

$$HNO_3(g) \rightarrow HNO_3(l) \quad (19)$$

The volumetric absorption rates of different species are given by Pradhan et al. [15] as:

$$Ra_{NO_2,L} = \underline{a}(H_{NO_2})^{3/2}\left[\frac{2}{3}(kD)_{NO_2}\right]^{1/2}(p^b_{NO_2} - p^i_{NO_2})^{3/2} \quad (20)$$

$$Ra_{N_2O_4,L} = \underline{a}H_{N_2O_4}[(kD)_{N_2O_4}]^{1/2}(p^i_{N_2O_4} - p^b_{N_2O_4}) \quad (21)$$

$$Ra_{N_2O_3,L} = \underline{a}H_{N_2O_3}[(kD)_{N_2O_3}]^{1/2}(p^i_{N_2O_3} - p^b_{N_2O_3}) \quad (22)$$

$$Ra_{HNO_2,L} = H_{HNO_2}(k_L\underline{a})_{HNO_2}(p^i_{HNO_2} - p^b_{HNO_2}) \quad (23)$$

The NO generated in the liquid phase due to HNO_2 decomposition and because of its lower solubility in liquid phase, gets desorbed. The rate of NO desorption depends upon the rate of HNO_2 decomposition in the liquid phase and is limited by the rate of absorption of NO_2, N_2O_3, N_2O_4 and HNO_2 in liquid. Thus, the rate of NO desorption can be written as:

$$Ra_{NO,L} = \frac{2}{3}(k_d(k_L\underline{a})^{2/3}[HNO_2]^{4/3} - k'_b[HNO_3]^2[NO]) \quad (24)$$

Carberry [29] in his work has shown that, for a given set of partial pressures of NO, NO_2 and N_2O_4, there exists a certain limiting concentration of nitric acid beyond which no absorption of N_2O_4 and NO_2 occurs. This heterogeneous equilibrium is mathematically presented in terms of parameter K_6:

$$K_6 = \frac{p^i_{NO}}{(p^b_{N_2O_4})^{3/2}} \quad (25)$$

Pradhan et al. [15] have given the correlation for the heterogeneous equilibrium constant as a function of temperature and HNO_3 concentration. The limiting partial pressures of NO_2, N_2O_3, and HNO_2 based on the heterogeneous equilibria can be written as:

$$p^b_{NO_2} = \left(\frac{p^b_{N_2O_4}}{K_2}\right)^{1/2} \quad (26)$$

$$p^b_{N_2O_3} = K_3(p^i_{NO})(p^i_{NO_2}) \quad (27)$$

$$p^b_{HNO_2} = (K_4 p^b_{NO} p^b_{NO_2} p^b_{H_2O})^{1/2} \quad (28)$$

Thus, the concentration of HNO_3 and HNO_2 in the liquid phase, together will limit the absorption of NOx gases in the water.

The NO generated in gas phase undergoes irreversible oxidation with oxygen. The oxidation reaction is expressed as:

$$2NO(g) + O_2(g) \xrightarrow{k_1} 2NO_2(g) \quad (29)$$

It is believed that the NO oxidation proceeds by dimerization of NO to N_2O_4. The various reactions take place in gas and liquid phases. The gas phase reactions and complex gas phase equilibria are represented below:

$$2NO_2(g) \overset{K_2}{\rightleftarrows} 2N_2O_4(g) \quad (30)$$

$$NO(g) + NO_2(g) \overset{K_3}{\rightleftarrows} N_2O_3(g) \quad (31)$$

$$NO(g) + NO_2(g) + H_2O(g) \overset{K_4}{\rightleftarrows} 2HNO_2(g) \quad (32)$$

$$3NO_2(g) + H_2O(g) \overset{K_5}{\rightleftarrows} 2HNO_3(g) + NO(g) \quad (33)$$

The NO oxidation rate constant k_1 [Eq. (29)] and gas phase equilibria constants are reported in the literature [16].

3. Mathematical model—absorber

A bubble cap tray column has been modeled for absorber to get HNO_2 and HNO_3 concentration profiles along the height of the column. The NOx gases from the cooler–condenser are introduced at the bottom of the column. The oxidizer is located below the lower section of the absorption column. The gases flow counter-current to the process water, entering from the top of the absorption column, to produce nitric acid. The decomposition of HNO_2, oxidation of NO with HNO_3 in the liquid phase and the HNO_2 oxidation with oxygen neglected previously [7,30] have been accounted in the model developed in this work.

The model developed accounts for: (i) gas phase equilibria [12,13], (ii) gas phase oxidation of NO to NO_2, (iii) formation of HNO_2 and HNO_3 [14], (iv) simultaneous absorption and chemical reaction of NO_2, N_2O_3 and N_2O_4 with water [15], (v) heterogeneous

gas–liquid equilibria [16], (vi) HNO_2 decomposition [21] and oxidation with oxygen in liquid phase [27] and (vii) desorption of NO preceded by its reaction with HNO_3 in the liquid phase.

The tray behavior is modeled by dividing the process into two parts: (i) the gases bubbling through the pool of liquid, considering it to be plug flow and (ii) the pool of liquid on the stage, considering it to be mixed flow.

The material balance for the gases bubbling through the pool of liquid is represented as:

1. Divalent nitrogen balance

$$\frac{dY^*_{NO}}{dz} = -\frac{S}{G}[k_1(p_{NO})^2 p_{O_2}\varepsilon_G - Ra_{NO,G} + Ra_{N_2O_3,G} + 0.5(Ra_{HNO_2,G} - Ra_{HNO_3,G})] \quad (34)$$

2. Total reactive nitrogen balance

$$\frac{dY^*_N}{dz} = -\frac{S}{G}[-Ra_{NO,G} + Ra_{NO_2,G} + 2Ra_{N_2O_3,G} + 2Ra_{N_2O_4,G} + Ra_{HNO_2,G} + Ra_{HNO_3,G}] \quad (35)$$

3. Water balance

$$\frac{dY^*_{H_2O}}{dz} = -\frac{S}{G}[Ra_{H_2O,G} + 0.5Ra_{HNO_2,G} + 0.5Ra_{HNO_3,G}] \quad (36)$$

4. Oxygen balance

$$\frac{dY^*_{O_2}}{dz} = -\frac{1}{2}\frac{S}{G}[k_1(p^o_{NO})^2 p^o_{O_2}\varepsilon_G + R_d\varepsilon_L] \quad (37)$$

The overall material balance for an absorption stage is given by the following equations:

(1) Reactive nitrogen balance

$$G(Y^*_{N,n-1} - Y^*_{N,n}) = L_nX^*_{N,n} - L_{n+1}X^*_{N,n+1} \quad (38)$$

(2) Water and water vapor balance

$$G(Y^*_{H_2O,n-1} - Y^*_{H_2O,n}) = L_n(1+0.5X^*_{N,n}) - L_{n+1}(1+0.5X^*_{N,n+1}) \quad (39)$$

To split the reactive nitrogen into HNO_2 and HNO_3, a liquid phase HNO_2 balance is taken as:

$$L_{n+1}X_{HNO_2,n+1} = L_nX_{HNO_2,n} + R_dV - (0.5Ra_{NO_2,L} + 2Ra_{N_2O_3,L} + Ra_{N_2O_4,L})V \quad (40)$$

The point rates of various components in gas phase need to be evaluated considering mass transfer resistance in the gas film. The volumetric rates of gas phase mass transfer are given as:

$$Ra_{NO,G} = (k_G\underline{a})_{NO}(p^i_{NO} - p_{NO}) \quad (41)$$

$$Ra_{NO_2,G} = (k_G\underline{a})_{NO_2}(p_{NO_2} - p^i_{NO_2}) \quad (42)$$

$$Ra_{N_2O_3,G} = (k_G\underline{a})_{N_2O_3}(p_{N_2O_3} - p^i_{N_2O_3}) \quad (43)$$

$$Ra_{N_2O_4,G} = (k_G\underline{a})_{N_2O_4}(p_{N_2O_4} - p^i_{N_2O_4}) \quad (44)$$

$$Ra_{HNO_2,G} = (k_G\underline{a})_{HNO_2}(p_{HNO_2} - p^i_{HNO_2}) \quad (45)$$

$$Ra_{HNO_3,G} = (k_G\underline{a})_{HNO_3}(p_{HNO_3} - p^i_{HNO_3}) \quad (46)$$

The interfacial partial pressures in Eqs. (41)–(46) can be expressed in terms of NO, NO_2, H_2O and HNO_3, with the help of equilibrium constants. Thus, interface equilibria can be written as:

$$K_2 = \frac{p^i_{N_2O_4}}{(p^i_{NO_2})^2} \quad (47)$$

$$K_3 = \frac{p^i_{N_2O_3}}{(p^i_{NO})(p^i_{NO_2})} \quad (48)$$

$$K_4 = \frac{(p^i_{HNO_2})^2}{(p^i_{NO})(p^i_{NO_2})(p^i_{H_2O})} \quad (49)$$

HNO_3 and H_2O are at their saturation concentrations at the interface. The vapor pressure of H_2O or HNO_3 is a function of temperature and nitric acid concentration:

$$p^i_{H_2O} = f[T, \text{conc}(HNO_3)] \quad (50)$$

$$p^i_{HNO_3} = f[T, \text{conc}(HNO_3)] \quad (51)$$

The volumetric rate for NO desorption in the liquid phase is given by Eq. (24). Since, NO desorbs rapidly from the liquid to the gas phase, the limiting partial pressure of NO due to heterogeneous equilibria can be assumed to be equal to the interface partial pressure as:

$$p^i_{NO} = p^b_{NO} \quad (52)$$

The gas phase composition is known but interface and liquid phase compositions are unknown. In order to get all the rates of gas and liquid phase mass transfer, NO and NO_2 balance at the interface is written as shown by the following equations:

NO balance at the interface

$$Ra_{NO,L} - Ra_{NO,G} = Ra_{N_2O_3,L} - Ra_{N_2O_3,G} + \frac{1}{2}(Ra_{HNO_2,L} - Ra_{HNO_2,G}) \quad (53)$$

NO_2 balance at the interface

$$Ra_{NO_2,G} - Ra_{NO_2,L} = 2(Ra_{N_2O_4,L} - Ra_{N_2O_4,G}) + Ra_{N_2O_3,L} - Ra_{N_2O_3,G} + \frac{1}{2}(Ra_{HNO_2,L} - Ra_{HNO_2,G}) \quad (54)$$

Eqs. (53) and (54) are coupled algebraic equations. In order to attain convergence under varied parametric conditions, it was found necessary to reduce them to a set of two equations in terms of p^i_{NO} and $p^i_{NO_2}$.

The concentration of product acid at the bottom plate is known. Knowing the HNO_2 concentration and liquid-side mass transfer coefficient, the liquid phase concentration of NO is evaluated with the help of Eq. (4). The decomposition rate of HNO_2 is evaluated from Eq. (11) and the desorption rate of NO is calculated from Eq. (24). The concentration of HNO_3 and H_2O at the interface is evaluated from their saturation concentration and temperature as shown in Eqs. (50) and (51). The interfacial partial pressure of N_2O_3, N_2O_4 and HNO_2 are converted in terms of p^i_{NO} and $p^i_{NO_2}$ with the help of Eqs. (47)–(49). From Eqs. (25)–(28) and (52), the limiting partial pressures of NO, NO_2, N_2O_3, N_2O_4 and HNO_2 are converted in terms of p^i_{NO} and $p^i_{NO_2}$. In Eqs. (53) and (54), the rates of various gas and liquid phase mass transfer are substituted from Eqs. (41)–(46) and (20)–(23). Thus, Eqs. (53) and (54) are converted into two unknowns namely, p^i_{NO} and $p^i_{NO_2}$ as shown in Appendix A. These non-linear algebraic equations are solved using Newton–Raphson in conjunction with Gauss–Jordon method. Knowing the interfacial partial pressures of NO, and NO_2, the interfacial and limiting partial pressures of N_2O_3, N_2O_4, HNO_2 are evaluated which in turn are used to determine the rates of gas and liquid phase mass transfer rates. Knowing the rates of gas phase mass transfer, the set of coupled differential Eqs. (34)–(37) is solved using Runge–Kutta fourth-order method over the weir height to evaluate Y^*_N, Y^*_{NO}, $Y^*_{H_2O}$ and $Y^*_{O_2}$. The partial pressures of all NOx components in the gas phase can be determined with the help of gas phase equilibria [7]. From Eq. (40), the HNO_2 concentration in the liquid phase on the next tray can

be determined, which then subtracted from total reactive nitrogen calculated from Eq. (38) to get the HNO_3 concentration in the liquid phase on the next stage. The empty section or the space between trays acts as an oxidizer for NO and the oxidizer model is well described by Chatterjee and Joshi [7].

4. Mathematical model—bleacher

The product acid from the absorption column is decolorized and made free from nitrous acid in the bleacher. This can be achieved by passing secondary air the air from compressor to the bleacher. The air helps in removing the dissolved nitrogen oxides, HNO_2 decomposition and its oxidation with oxygen. Since the partial pressure of nitrogen oxides in gas phase is comparatively low, the absorption of nitrogen oxides can be neglected, to simplify the model. The decomposition and oxidation of HNO_2 were discussed earlier.

During bubbling of the air through the pool of liquid on the tray, the decomposition and oxidation of HNO_2 with the evolution of NO in the gas phase and its subsequent oxidation with oxygen take place. The gases are considered to flow in plug flow manner while bubbling through the liquid pool. The material balance across a differential height in the liquid pool for NO and oxygen balance can be written as:

$$\frac{dY_{NO}}{dz} = \frac{S}{G}\left[\frac{2}{3}R_d - k_1(p_{NO})^2 p_{O_2}\varepsilon_G\right] \quad (55)$$

$$\frac{dY_{O_2}}{dz} = -\frac{1}{2}\frac{S}{G}[R_o + k_1(p_{NO})^2 p_{O_2}\varepsilon_G] \quad (56)$$

Eqs. (55) and (56) can be solved simultaneously with the help of fourth-order Runge–Kutta method over the weir height. Thus, the partial pressures of NO and O_2 can be obtained after the liquid pool. The evolved NO is oxidized in the gas space between the two plates which acts as an oxidizer. The oxidizer model is well described by Chatterjee and Joshi [7].

The liquid phase on the tray is considered to be back-mixed. The liquid phase balance for nitric and nitrous acid can be written as shown in Eqs. (57) and (58).

$$L_{n+1}X_{HNO_2,n+1} = L_nX_{HNO_2,n} + (R_d + R_o)V \quad (57)$$

$$L_{n+1}X_{HNO_3,n+1} = L_nX_{HNO_3,n} - \frac{1}{3}R_dV - R_oV \quad (58)$$

The rate of HNO_2 decomposition, R_d and HNO_2 oxidation, R_o are taken from Eqs. (11) and (14) respectively. Eqs. (57) and (58) can be solved simultaneously to get the concentrations of HNO_2 and HNO_3 in liquid phase. The stages are numbered from bottom to top of the column. The acid from the bottom plate of the absorber enters the top plate of the bleacher column. The calculations are started at the bottom of the bleacher column, assuming acid concentration in the liquid phase.

5. Results and discussions

The absorber model developed in this work predicts the HNO_3 and HNO_2 concentration profiles along the height of the bubble cap column. The process parameters of an operating plant used for the model validation are described in the works of Chatterjee and Joshi [7]. Fig. 1A and B shows an appreciable match in the concentration profile of HNO_3 and HNO_2 respectively, which is well within 5% deviation from the plant data. Thus the model developed in this work successfully predicts the HNO_2 composition along the length of the absorption column, in addition to the concentration profile of HNO_3.

Thus the decomposition kinetics of HNO_2 plays an important role in the absorber model. As earlier reported by Komiyama and Inoue [21] at high nitric acid concentration the reverse reaction

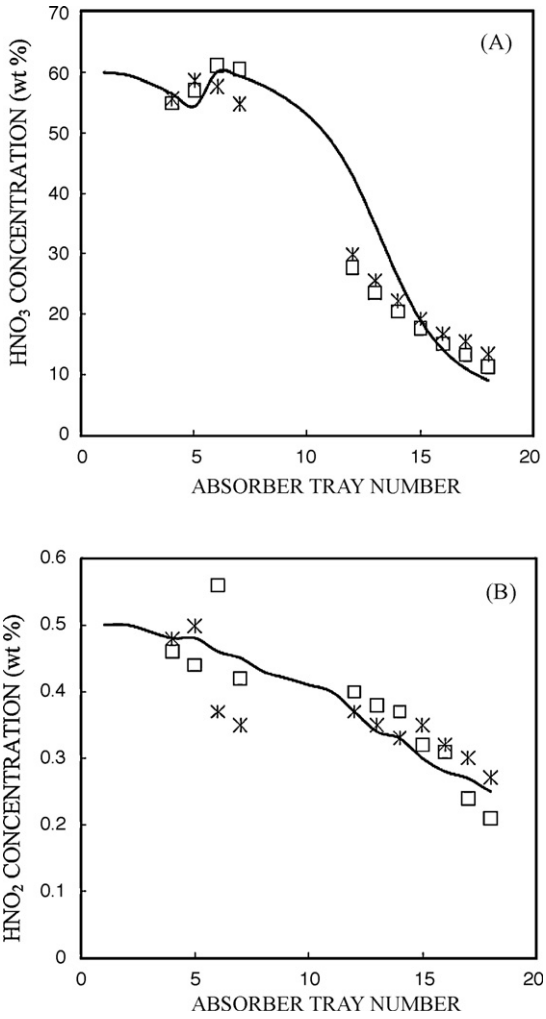

Fig. 1. (A) Concentration profile of HNO_3 in liquid phase along the length of the absorber (□, plant data case 2 [7]; ✳, plant data case 3 [7]; —, model predicted). (B) Concentration profile of HNO_2 in liquid phase along the length of the absorber (□, plant data case 2 [7]; ✳, plant data case 3 [7]; —, model predicted).

of decomposition of HNO_2 is favored. The model developed in this work is in agreement to these observations and are well established through the model validation results presented in Fig. 1A and B.

It can be observed from Fig. 1B that, the HNO_2 concentration falls less rapidly in the bottom trays of the absorption column, where the concentration of HNO_3 in liquid phase is 40–60 wt.%, as observed in Fig. 1A. At this concentration, the NO solubility in the liquid phase is high and hence the HNO_2 decomposition rate decreases. Therefore, the reverse reaction of HNO_2 decomposition is more favorable at high nitric acid concentration. As the concentration of HNO_3 in the liquid phase falls, the HNO_2 decomposes rapidly and thus, there is a fall in HNO_2 concentration at the top trays of the absorber.

The present model is also validated from the plant data reported by Guitternez-Canas et al. [30]. The reported data for the absorber column is for a 330 tpd of nitric acid plant (100% basis) from a fertilizer production facility. The nitrous gases from the cooler–condenser are fed to absorption column and the condensed stream which contains HNO_2 and HNO_3 is fed at an intermediate absorption stage. The column is equipped with sieve tray as internals. The correlations for the mass transfer coefficients for sieve trays are taken from Zuiderweg [31]. The absorption is carried out at 300 kPa pressure. Other process parameters are detailed in Guitternez-Canas et al. [30]. They have compared the absorption column performance with the transport model and the equilibrium

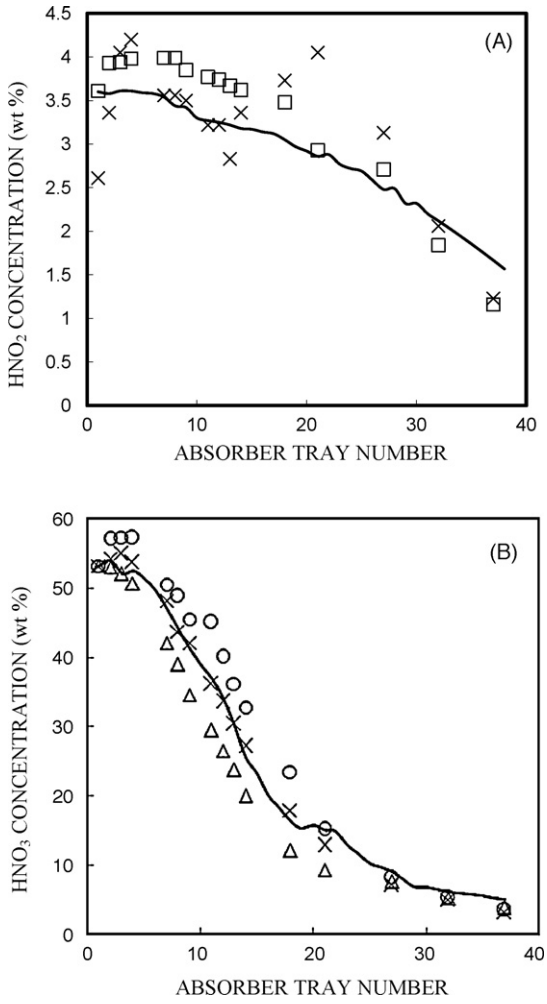

Fig. 2. (A) Concentration profile of HNO_2 in liquid phase along the length of the absorber (×, experimental data [30]; ○, equilibrium model [30]; —, present model). (B) Concentration profile of HNO_3 in liquid phase along the length of the absorber (○, experimental data [30]; △, equilibrium model [30]; ×, transport model [30]; —, present model).

model. The equilibrium model takes into account the thermodynamic equilibrium at each stage with sufficient time provided. Whereas, transport model takes into account the kinetic and mass transfer analysis. From Fig. 2A, it is clear that the HNO_2 concentration decreases along the height of the absorber. From Fig. 2A and B, it is seen that the model is in good agreement with plant data with deviation of 10%.

As can be seen from Fig. 3, the present model predicts the concentration profile of HNO_3 more closely compared to the previous model. In particular, (a) the present model captures the maxima in concentration in the tray number range of 4–6; (b) the present model eliminates the discontinuity in the trays 13–15 and (c) the present model gives much superior predictions in the tray range of 10–20. This aids in evaluating a better estimation, for outlet NOx composition. Optimization studies for the nitric acid plant can benefit from the development of this model, as it predicts the behavior of the absorber more with a deviation of 5% as compared to a deviation of 10% in the previous model [7]. Thus the prediction of this model has improved by 100% when compared with the previous model developed, thereby increasing the accuracy of costing with this model. The contribution of the absorber in the total annualized cost of nitric acid is 5.5%; thereby, the improvement in model prediction has a very significant role.

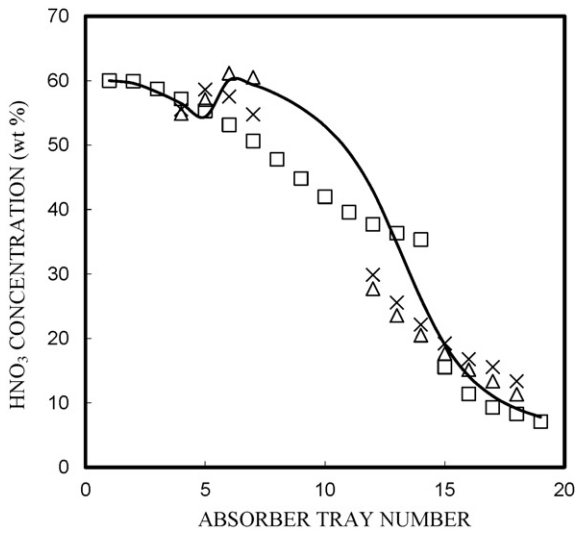

Fig. 3. Concentration profile of HNO_3 in liquid phase indicating the effect of HNO_2 decomposition (△, plant data case 2 [7]; ×, plant data case 3 [7]; □, absorber model [7]; —, present model).

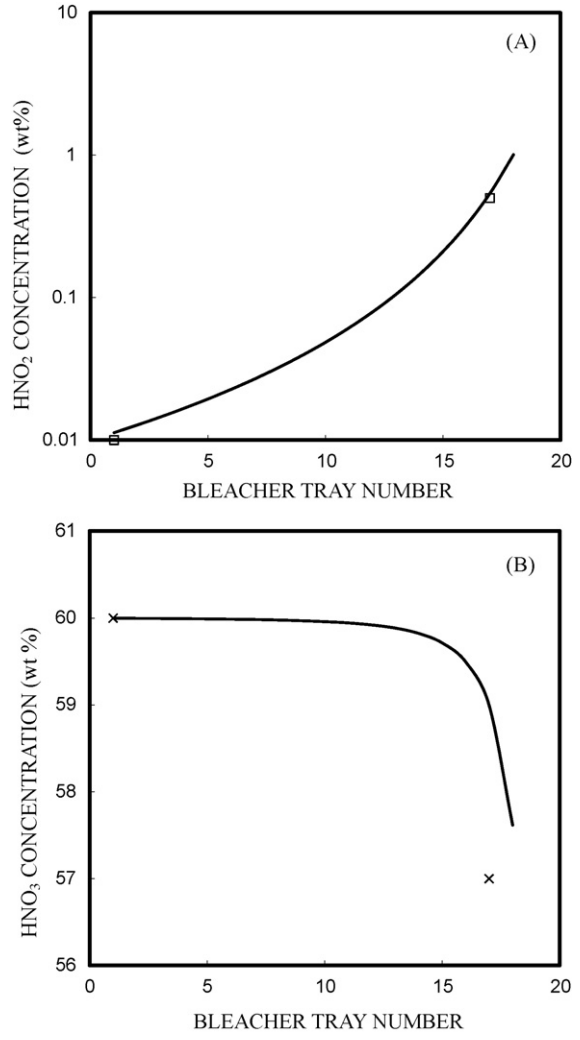

Fig. 4. (A) Concentration profile of HNO_2 in liquid phase along the length of the bleacher (□, plant data; —, model predicted). (B) Concentration profile of HNO_3 in liquid phase along the length of the bleacher (×, plant data; —, model predicted).

For validating the bleacher model, the model predictions are compared with the plant data of Chatterjee and Joshi [7]. Air is passed through the bottom of the bleacher to remove dissolved gases and aid in HNO_2 decomposition. The oxygen has solubility in the liquid phase [27] and is capable of oxidizing the nitrous acid in the liquid phase. Considering both these aspects, the concentration of HNO_2 and HNO_3 obtained is shown in Fig. 4A and B. The concentration of HNO_2 in the liquid phase on the tray increases whereas the HNO_3 concentration decreases. At the bottom of the bleacher, HNO_2 concentration in the liquid phase is less (i.e. 0.01 wt.%) compared to the top of the bleacher column (0.57 wt.%). Thus, the rate of HNO_2 decomposition is small at the bottom stages and so is the rate of NO evolution. There is no absorption taking place on the stages of the bleacher column as NOx gases composition is small. Only desorption of NO, HNO_2 decomposition and oxidation in the liquid phase are important.

6. Conclusions

The mathematical model developed in this work for the absorber and the bleacher includes: (i) kinetics of liquid phase decomposition of HNO_2, (ii) heterogeneous equilibria between NO, N_2O_3, N_2O_4 and HNO_3, HNO_2, (iii) the effects of maximum permissible concentration of nitric and nitrous acid in NOx absorption and (iv) the assumption of complete liquid phase decomposition of HNO_2 is relaxed in the present work.

There is good agreement between the model's predictions against the data reported in the published literature. The reversibility of HNO_2 decomposition at high nitric acid concentration is important, which is clear from the results obtained in the present work. Any NOx absorption system should take into account the liquid phase HNO_2 decomposition kinetics.

Appendix A.

The NO balance at the interface from Eq. (53) can be converted into two unknowns namely, p^i_{NO} and $p^i_{NO_2}$ as described below:

The rates of various NOx components for gas phase mass transfer from Eqs. (41)–(46) and liquid phase mass transfer rates from Eqs. (20)–(24) are substituted and modified in Eqs. (53) and (54). The interfacial and bulk partial pressures of NO, NO_2, N_2O_3, N_2O_4 and HNO_2 are converted into p^i_{NO} and $p^i_{NO_2}$. The resulting equations are as shown in Eqs. (A1) and (A2).

$$A_1 + A_2 - A_3 p^i_{NO} - A_4 p^i_{NO} p^i_{NO_2} + A_5 (p^i_{NO})^{4/3} + A_6 - A_7 (p^i_{NO} p^i_{NO_2})^{1/2} + A_8 (p^i_{NO})^{2/3} = 0 \quad \text{(A1)}$$

where

$$A_1 = \frac{2}{3}(k_d (k_L a)^{2/3} [HNO_2]^{4/3} - k'_b [HNO_3]^2 [NO])$$

$$A_2 = (k_G a)_{NO} p_{NO}$$

$$A_3 = (k_G a)_{NO}$$

$$A_4 = K_3 (a H_{N_2O_3} ((kD)_{N_2O_3})^{1/2} + (k_G a)_{N_2O_3})$$

$$A_5 = a H_{N_2O_3} ((kD)_{N_2O_3})^{-1/2} K_3 K_2^{-1/2} K_6^{-1/3}$$

$$A_6 = (k_G a)_{N_2O_3} p_{N_2O_3}$$

$$A_7 = \frac{1}{2} H_{HNO_2} (k_L a)_{HNO_2} (K_4 p^i_{H_2O})^{1/2}$$

$$A_8 = \frac{1}{2} H_{HNO_2} (k_L a)_{HNO_2} (K_4 p^b_{H_2O})^{1/2} K_2^{-1/2} K_6^{-1/3}$$

Similarly, the NO_2 balance at interface can be written as:

$$B_1 - B_2 p^i_{NO_2} - B_3 (p^i_{NO_2} - B_4 (p^i_{NO})^{1/3})^{3/2} - B_5 (p^i_{NO_2})^2 + B_6 (p^i_{NO})^{2/3} + B_7 - B_8 p^i_{NO} p^i_{NO_2} + B_9 (p^i_{NO})^{4/3} - B_{10} (p^i_{NO} p^i_{NO_2})^{1/2} = 0 \quad \text{(A2)}$$

where

$$B_1 = (k_G a)_{NO_2} p_{NO_2}$$

$$B_2 = (k_G a)_{NO_2}$$

$$B_3 = a (H_{NO_2})^{3/2} \left(\left(\frac{2}{3} kD \right)_{NO_2} \right)^{1/2}$$

$$B_4 = K_2^{-1/2} K_6^{-1/3}$$

$$B_5 = 2a H_{N_2O_4} ((kD)_{N_2O_4})^{1/2} K_2 + 2 (k_G a)_{N_2O_4} K_2$$

$$B_6 = 2a H_{N_2O_4} ((kD)_{N_2O_4})^{1/2} K_6^{-2/3} + \frac{1}{2} H_{HNO_2} (k_L a)_{HNO_2} (K_4 p^b_{H_2O})^{1/2} K_2^{-1/2} K_6^{-1/3}$$

$$B_7 = 2 (k_G a)_{N_2O_4} p_{N_2O_4}$$

$$B_8 = (K_3 a H_{N_2O_3} ((kD)_{N_2O_3})^{1/2} + (k_G a)_{N_2O_3} K_3)$$

$$B_9 = a H_{N_2O_3} ((kD)_{N_2O_4})^{1/2} K_3 K_2^{-1/2} K_6^{-1/3}$$

$$B_{10} = \frac{1}{2} H_{HNO_2} (k_L a)_{HNO_2} (K_4 p^i_{H_2O})^{1/2}$$

References

[1] P.J. Hoftizer, F.J.G. Kwanten, in: G. Nonhabel (Ed.), Absorption of Nitrous Gases, Gas Purification Processes for Air Pollution Control, Newnes Butterworths, London, 1972.
[2] C. Matassa, E. Tonca, Basic Nitrogen Compounds, Chemical Publishing Co., New York, 1973.
[3] T.K. Sherwood, R.L. Pigford, C.R. Wilke, Mass Transfer, McGraw-Hill, New York, 1975.
[4] J.J. Carberry, Chemical and Catalytic Reaction Engineering, McGraw-Hill, New York, 1976.
[5] G.D. Honti, in: Keleetic (Ed.), Various Processes for the Manufacture of Commercial Grade Nitric Acid, Nitric Acid and Nitrates-Fertilizer Science and Technology Series, Marcel Dekker, New York/Basel, 1985.
[6] J.B. Joshi, V.V. Mahajani, V.A. Juvekar, Absorption of NOx gases, Chem. Eng. Commun. 33 (1985) 1–92.
[7] I.B. Chatterjee, J.B. Joshi, Modelling, simulation and optimization: mono pressure nitric acid process, Chem. Eng. J. 138 (2008) 556–577.
[8] R.M. Counce, J.J. Perona, A mathematical model for nitrogen oxide absorption in a sieve plate column, Ind. Eng. Chem. Process. Des. Dev. 19 (1980) 426–431.
[9] D.N. Miller, Mass transfer in nitric acid absorption, AIChE J. 33 (1987) 1351–1357.
[10] W. Weisweiler, K. Eidam, M. Thiemann, E. Scheibler, K.W. Wieand, Absorption of NO/NO_2 in nitric acid, Chem. Eng. Technol. 13 (1990) 97–101.
[11] V. Sobotka, Modeling of an absorption column for nitric acid manufacture, Int. Chem. Eng. 13 (1973) 718–727.
[12] G. Emig, K. Wohlfahrt, U. Hoffmann, Absorption with simultaneous complex reactions in both phases, demonstrated by the modeling and calculation of a counter current flow column for the production of nitric acid, Comput. Chem. Eng. 3 (1979) 143–150.
[13] F.T. Shadid, D. Handley, Absorption of nitrogen oxides using a baffle tray, Chem. Eng. Res. Dev. 67 (1989) 185–192.
[14] N.J. Suchak, J.B. Joshi, Simulation and optimization of NOx absorption system in nitric acid manufacture, AIChE J. 40 (1994) 944–956.

[15] M.P. Pradhan, N.J. Suchak, P.R. Walse, J.B. Joshi, Multicomponent gas absorption with multiple reactions: modeling and simulation of NOx absorption in nitric acid manufacture, Chem. Eng. Sci. 52 (1997) 4569–4591.
[16] N.J. Suchak, K.R. Jethani, J.B. Joshi, Modeling and simulation of NOx absorption in pilot-scale packed columns, AIChE J. 37 (1991) 323–339.
[17] E. Decanini, G. Nardini, A. Paglianti, Absorption of nitrogen oxides in columns equipped with low-pressure drops structured packings, Ind. Eng. Chem. Res. 39 (2000) 5003–5011.
[18] B. Hupen, E.Y. Kenig, Rigorous modeling of NOx absorption in tray and packed columns, Chem. Eng. Sci. 60 (2005) 6462–6471.
[19] E. Abel, H. Schmid, Kinetik der salpetrigen saure I. Einleitung und ubersicht II. Orientierende versuche, Z. Phys. Chem. 132 (1928) 55–77.
[20] E. Abel, H. Schmid, Kinetik der salpetrigen saure III. Kinetik des Salpetrigsaurez-erfalls, Z. Phys. Chem. 134 (1928) 279–300.
[21] H. Komiyama, H. Inoue, Reaction and transport of nitrogen oxides in nitrous acid solutions, J. Chem. Eng. Jpn. 11 (1978) 25–32.
[22] T.W.J. Taylor, E.W. Wignall, J.F. Cowley, The decomposition of nitrous acid in aqueous solution, J. Chem. Soc. (1927) 1923–1927.
[23] V.H. Veley, The conditions of the formation and decomposition of nitrous acid, Chem. News LXVI, 1715 (1892) 175–177.
[24] Saposhnikov, J. Russ. Phys. Chem. Soc. 32 (1900) 375–378.
[25] Saposhnikov, J. Russ. Phys. Chem. Soc. 33 (1901) 306–308.
[26] L.Ya. Tereshchenko, V.P. Panov, M.E. Pozin, Driving force of oxidation of nitrous oxide by dilute nitric acid, Russ. J. Phys. Chem. (1972) 2765–2767.
[27] L.Ya. Tereshchenko, V.P. Panov, M.E. Pozin, Influence of the composition of the liquid phase on oxidation of nitric oxide, Russ. J. Phys. Chem. (1972) 2765–2767.
[28] A. Chacuk, J.S. Miller, M. Wilk, S. Ledakowicz, Intensification of nitrous acid oxidation, Chem. Eng. Sci. 62 (2007) 7446–7453.
[29] J.J. Carberry, Some remarks on chemical equilibrium and kinetics in the nitrogen dioxide–water system, Chem. Eng. Sci. 9 (1959) 189–194.
[30] C. Guitternez-Canas, P.L. Arias, J.A. Legarreta, Industrial nitrogen oxides absorption simulation, Comput. Chem. Eng. 13 (1989) 985–1002.
[31] F.J. Zuiderweg, Sieve trays: a view on the state of the art, Chem. Eng. Sci. 37 (1982) 1441–1464.